The cell adhesion molecule Roughest depends on β_{Heavy}-spectrin during eye morphogenesis in *Drosophila*

Hyun-Gwan Lee, Daniela C. Zarnescu*, Bryce MacIver‡ and Claire M. Thomas§

Department of Biology, Department of Biochemistry and Molecular Biology, Eberly College of Science, The Pennsylvania State University, University Park, PA 16802, USA

*Present address: Molecular and Cellular Biology, University of Arizona, Life Sciences South, Tucson AZ 85721, USA

‡Present address: Department of Medicine, Division of Nephrology, Beth Israel Deaconess Medical Center, Harvard University, Boston, MA 02215, USA

§Author for correspondence (clairet@psu.edu)

Accepted 5 November 2009
Journal of Cell Science 123, 277-285 Published by The Company of Biologists 2010
doi:10.1242/jcs.056853

Summary

Cell junctions have both structural and morphogenetic roles, and contain complex mixtures of proteins whose interdependencies are still largely unknown. Junctions are also major signaling centers that signify correct integration into a tissue, and modulate cell survival. During *Drosophila* eye development, the activity of the immunoglobulin cell adhesion molecule Roughest (also known as Irregular chiasm C-roughest protein) mediates interommatidial cell (IOC) reorganization, leading to an apoptotic event that refines the retinal lattice. Roughest and the cadherin-based zonula adherens (ZA) are interdependent and both are modulated by the apical polarity determinant, Crumbs. Here we describe a novel relationship between the Crumbs partner β_{Heavy}-spectrin (β_H), the ZA and Roughest. Ectopic expression of the C-terminal segment 33 of β_H (βH33) induces defects in retinal morphogenesis, resulting the preferential loss of IOC. This effect is associated with ZA disruption and Roughest displacement. In addition, loss-of-function *karst* and *roughest* mutations interact to cause a synergistic and catastrophic effect on retinal development. Finally, we show that β_H coimmunoprecipitates with Roughest and that the distribution of Roughest protein is disrupted in *karst* mutant tissue. These results suggest that the apical spectrin membrane skeleton helps to coordinate the Cadherin-based ZA with Roughest-based morphogenesis.

Key words: *Drosophila*, Cell adhesion, Apoptosis, Spectrin, Membrane skeleton, Crumbs, IrreC, Roughest

Introduction

Cell adhesion complexes have both structural and morphogenetic roles, holding cells together while still facilitating morphogenetic rearrangements. The factors determining the level of adhesion are complex and manifold, including the type and combination of adhesion molecules expressed, level of expression, turnover rates, modulation by regulatory factors and cytoskeletal engagement. The coordination of these properties is not well understood but certainly involves multiple pathways that are integrated at the surface to produce the appropriate properties for any particular developmental context. Junctions are also major signaling centers that signify correct integration into a tissue and modulate cell survival (Cabodi et al., 2004; Hollande et al., 2005). During normal development, cell survival is predicated upon an integrative assessment of the outputs from multiple pro- and anti-apoptotic pathways that both prevent abnormal proliferation and promote selective loss of cells. These act in concert to regulate and create specific structure and form.

Fly eyes are composed of strikingly regular, crystalline arrays of photoreceptor clusters (ommatidia) separated by a grid of pigment and bristle cells. During pupariation in *Drosophila*, cadherin and immunoglobulin cell adhesion molecule (Ig-CAM) adhesion systems interact to refine the retinal lattice to produce this regularity. Over a period of about 24 hours undifferentiated interommatidial cell (IOC) precursors compete for survival by making contacts with differentiated primary pigment cells. During this period IOC rearrange into a single row of pigment and bristle cells surrounding each ommatidium. A round of apoptosis then removes excess cells to set the final number of IOC. The Ig-CAM proteins Roughest (also known as Irregular chiasm C-roughest protein) and Hibris mediate IOC-primary cell contact and morphogenesis (Carthew, 2007; Tepass and Harris, 2007). The cadherin-based zonula adherens (ZA) has also been shown to be essential for this morphogenesis, for Roughest localization and for correct apoptosis (Grzeschik and Knust, 2005). Close coordination of these two adhesion systems is further indicated by the observations that Roughest modulates the ZA (Bao and Cagan, 2005). The mechanism by which this coordination is achieved is currently unknown.

The integral membrane protein Crumbs has essential roles in determining apical membrane identity, cell survival, and in the formation and stability of the ZA (Assemat et al., 2008; Martin-Belmonte et al., 2007; Grawe et al., 1996; Tepass, 1996). The cytoplasmic domain of Crumbs contains two functionally distinct sequences: a PDZ-domain binding site and a FERM-domain binding site. The former binds to the apical polarity protein Stardust and is required for the development of the apical pole (Klebes and Knust, 2000; Wodarz et al., 1995). The latter recruits β_{Heavy}-spectrin (β_H) (Medina et al., 2002) and is required for stabilization of the ZA (Klebes and Knust, 2000). Loss-of-function *karst* mutations in the locus encoding β_H cause cell shape defects that are accompanied by a loss of ZA integrity, but no loss of polarity (Zarnescu and Thomas, 1999).

β_H is part of the spectrin-based membrane skeleton, a two-dimensional spectrin-F-actin network that is associated with various cellular membranes. Through scaffolding (Bennett and Baines, 2001; De Matteis and Morrow, 2000) and transport (Johansson et al., 2007; Kizhatil et al., 2007a; Kizhatil et al., 2007b; Muresan et al., 2001;

Phillips and Thomas, 2006; Stabach et al., 2009) activities, spectrins can variously stabilize proteins at the membrane, nucleate protein complexes and modulate protein delivery and recycling. The Crumbs-β_H complex has been implicated in the development and maintenance of the apical domain via the modulation of endocytosis in both loss-of-function and gain-of-function experiments (Pellikka et al., 2002; Williams et al., 2004). This activity appears to be centered on the C-terminal segment 33 of β_H (βH33), the overexpression of which causes membrane growth and the sequestration of Dynamin (Williams et al., 2004). In some tissues, expression of βH33 also induces apoptosis (Williams et al., 2004). These phenotypes are β_H specific, because overexpression of the equivalent region of the basolateral β-spectrin does not have this effect (Williams et al., 2004). Modulation of endocytosis or recycling of junctional proteins through interactions with segment 33 of β_H might thus provide the normal mechanism whereby the ZA is stabilized.

Here, we further characterize the effects of βH33 in the developing eye. We find that βH33 expression preferentially results in the loss of IOC. We further show that these defects in morphogenesis are associated with fragmentation of the ZA and disruption of the Ig-CAM Roughest. In addition, we show that β_H genetically and physically interacts with Roughest to maintain its wild-type distribution. Because β_H also supports the ZA, we suggest that the activity of β_H serves to coordinate the ZA and Roughest/Ig-CAM adhesion systems.

Results

Similar to other β-spectrin isoforms β_H has a C-terminal domain (segment 33 in β_H; βH33) that contains a pleckstrin homology (PH) domain (ii in Fig. 1). These PH domains contribute to membrane association by means of their direct binding to phosopholipids, most significantly phosphatidylinositol 4,5-bisphosphate (Ferguson et al., 2000; Godi et al., 1998; Hyvonen et al., 1995; Lietzke et al., 2000; Lombardo et al., 1994; Zhang et al., 1995). Expression of βH33 causes membrane extensions in tubular primary epithelia (e.g. embryonic salivary glands and trachea), and apoptosis in planar primary epithelia (e.g. embryonic ectoderm and imaginal discs). The membrane extension activity requires regions i-iii of βH33; whereas, the induction of apoptosis requires only regions ii-iii. Deletion of the PH domain prevents both phenotypes (Fig. 1) (Williams et al., 2004). We compared the lipid-binding specificity of the β_H PH domain with the closely related PH domain from β-spectrin, which does not have these dominant effects. There are no differences that can readily explain the dominant effects of βH33 through phospholipid sequestration (supplementary material Fig. S1). We were also unable to detect any perturbation in the cell cycle upon βH33 expression that might account for its apoptotic effects (supplementary material Fig. S2). This result further suggests that βH33 does not affect the supply of undifferentiated precursor cells (see also below). Instead, βH33 might perturb an activity such as cell adhesion, leading indirectly to apoptosis.

Mild expression of βH33 results in preferential loss of pigment cells

Using the GMR-Gal4 driver (GMR>βH33), βH33 causes a rough eye phenotype that exhibits the typical temperature dependence that arises from the temperature-sensitive activity of Gal4 in fly cells. Previous results suggest that this eye phenotype is largely due to a loss of cells via apoptosis (Williams et al., 2004); however, the origin of this phenotype is unknown. Using two different drivers to induce a mild βH33 phenotype at ~22°C (GMR-Gal4 and 69B-Gal4; Fig. 2F,G), we noticed that pigments cells are preferentially absent in sections of the adult retina, whereas bristles are seen to be lost in SEM images (Fig. 2B,C). Pigment and bristle cells are the last to differentiate during eye development, and this sensitivity to βH33 expression suggests that these cell types, or their precursors, might have a particular dependence on β_H-spectrin.

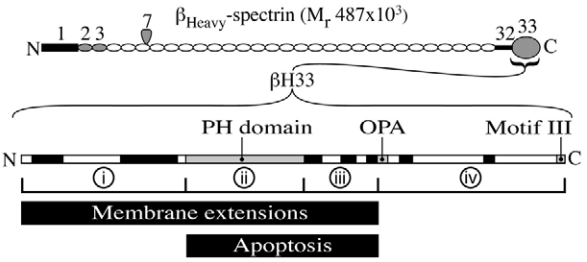

Fig. 1. Schematic diagram of β_{Heavy}-spectrin and βH33. Top: β_H, most of which is composed of spectrin repeats (ellipses). Known or predicted regions of functionality are indicated by their segment numbers: 1, F-actin binding domain; 2,3, $\alpha\beta_H$ dimer nucleation site; 7, SH3 domain; 32, $(\alpha\beta_H)_2$ tetramerization domain; 33, βH33 (for a review see Bennett and Baines, 2001). Bottom: an enlarged schematic of βH33: PH, pleckstrin homology domain; OPA, polyglutamine repeat; motif III, lysine rich C-terminus; Black shading indicates regions with ≥50% identity with the mosquito orthologue. βH33 binds to the membrane, causing membrane extension and apoptosis (see Williams et al., 2004). Deletion analysis has shown that the PH domain, ii, is required for all these activities. A construct comprising regions i, ii and iii, inhibits endocytosis and induces apoptosis. A smaller construct comprising regions ii and iii induces only apoptosis (see Williams et al., 2004).

Interommatidial cells are preferentially lost during pupation upon βH33 expression

During mid-pupariation, undifferentiated interommatidial cell (IOC) precursors give rise to the secondary and tertiary pigment cells and bristle cells that are lost upon βH33 expression (see Fig. 2). During this period the IOCs rearrange position to lie in a single row between the ommatidia as an essential prerequisite for a normal round of apoptosis that eliminates excess cells from the retina (Fig. 3A-D). The Ig-CAM, Roughest mediates this event (Carthew, 2007; Tepass and Harris, 2007).

To see whether the absence of IOCs in adult GMR>βH33 eyes results from disruption of IOC morphogenesis we examined discs expressing the ZA marker α-catenin, labeled with GFP (α-catenin::GFP). Up until IOC morphogenesis the retina appears relatively normal, although we do see more irregular cell shapes and some interruptions in the normally continuous ZA at this stage (Fig. 3E,F). To verify that βH33 has not caused any cell loss by this stage, we counted the IOCs in representative images from several discs and normalized their number to the number of cone cell clusters present. Control (GMR-Gal4) discs had an average of 9.59±0.37 IOCs/ommatidium (10 discs, 287 ommatidia) and GMR-Gal4>βH33 discs had an average of 10.27±0.42 IOCs/ommatidium (12 discs, 225 ommatidia). This difference is not significant (P=0.284; t-test) and confirms that βH33 does not induce significant cell loss prior to this stage. However, as IOC development proceeds increased disruption of the ZA becomes evident and many cells are lost, often resulting in no IOCs between adjacent clusters (Fig. 3G,H). In addition, some primary pigment cells are lost resulting in fusion of neighboring ommatidia (Fig. 3H). This effect has a strong gradient along the anterior-posterior axis with the posterior

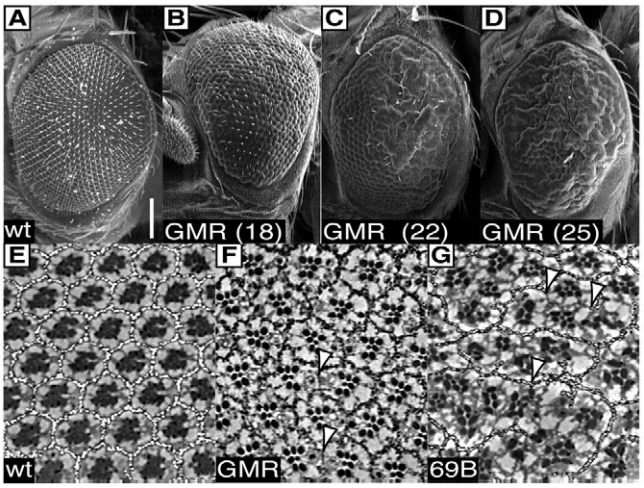

Fig. 2. βH33 expression causes preferential loss of interommatidial cells. (**A-D**) Scanning electron micrographs of adult eyes. (A) Wild-type eye. Scale bar: 100 µm. (B-D) Eyes of GMR>βH33 flies raised at 18°C, 22°C and 25°C, respectively. The βH33 rough eye phenotype is associated with merging of neighboring lenses and an absence of bristles. (**E-G**) Phase contrast images of sectioned eyes. (E) Section through a wild-type eye. (F,G) Mild expression of βH33 (~22°C) in GMR>βH33 (F) and 69B>βH33 (G) causes a selective loss of interommatidial cells and disrupts ommatidial morphology. Arrowheads indicate examples of gaps in the pigment cell grid. Note that the pigment cells are more prominent with the 69B-Gal4 driver because the *P{w*$^{+}$*}* marker in this transgene produces more pigment.

regions being most affected. Additional morphologies that are seen include inappropriate cone cell arrangements, cells that are not properly arranged in the tertiary cell niche and multiple rows of IOCs between some ommatidia where excessive IOC loss has not occurred (Fig. 3I,J). The wild-type cellular organization in the retina is established through differential cell adhesion together with tensile forces (Bao and Cagan, 2005; Kafer et al., 2007). Our data indicate that expression of βH33 has a major effect on the ability of cells in the retina to form and maintain these normal relationships.

Localization of β_H and βH33 during eye morphogenesis

To gain insight into the normal role of β_H during eye morphogenesis, we stained for β_H in a GMR>α-catenin::GFP background. Typically β_H is distributed at or very near the ZA with additional apical surface accumulation in some cell types (Zarnescu and Thomas, 1999), or during morphogenesis (Thomas and Kiehart, 1994). During larval eye development the highest levels of β_H are present at the ZA in photoreceptor cell clusters in the third instar eye disc (Thomas et al., 1998).

In the pupal eye, β_H is found across the apical domain of all cells at all stages. The level of this distribution varies relative to that at (or near) the ZA, sometimes being very faint, sometimes being the dominant distribution (e.g. Fig. 4C). In photoreceptor cells, β_H is highly enriched at all stages in the ZA and/or the apical domain where it initially colocalizes with α-catenin, but then becomes restricted to at the apical surface between the ZAs (Fig. 4B′-F′). There also appears to be low levels of β_H present on the lateral membranes and in short arcs at the basal domain at various stages, suggesting that the apical restriction of β_H is not absolute.

In non-photoreceptor cells, the distribution of β_H dynamically changes in its relationship with the ZA. Throughout cell rearrangement, β_H colocalizes with α-catenin at the ZA where it is at its highest levels in ZA involving the cone cells (Fig. 4A,B). At the stage when the IOC-primary cell boundaries begin to curve towards the primary cells and the ZA between neighboring IOC will shortly disappear (Bao and Cagan, 2005), β_H is prominent on the apical surface (Fig. 4C). This distribution is short lived and β_H

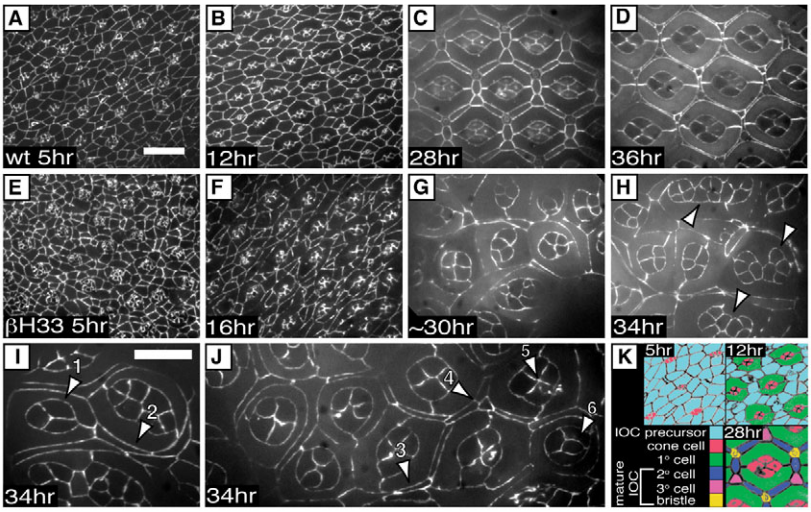

Fig. 3. Interommatidial cells are preferentially lost during eye morphogenesis when βH33 is expressed. Mid-pupal eye discs expressing α-catenin::GFP (GMR-Gal4>α-catenin::GFP; 25°C) to label the ZA. Each image is a maximum projection of a short stack of images through the level of the ZA acquired through the pupal membrane of live individuals. (**A-D**) Wild-type eye discs at approximately 5, 12, 28 and 36 hours after pupariation. (**E-H**) GMR>βH33 + α-catenin::GFP eye discs at approximately 5, 16, 30 and 34 hours after pupariation, respectively. Conspicuous loss of IOCs occurs during the time of normal IOC morphogenesis. Primary cells are often lost, resulting in fusion of neighboring cone cell clusters (arrowheads). This is accompanied by cell shape abnormalities and ZA fragmentation. (**I,J**) Higher magnification views illustrating further defects in morphogenesis in GMR>βH33 retina. Arrowheads: 1, loss of a cone cell; 2, 3, multiple rows of IOC between clusters; 4, inappropriate secondary-secondary cell contact at a tertiary cell niche; 5, equalized cone cell adhesion resulting in loss of central two-cell interface; 6, cone cell with reduced surface area enwrapped by two neighbors, possibly an intermediate to the situation indicated by arrowhead 1 in I. (**K**) Key to cell types. Regions copied from B, C and D were inverted and the different cell types colored as indicated in the key (1°, primary; 2°, secondary; 3°, tertiary). Scale bars: 10 µm.

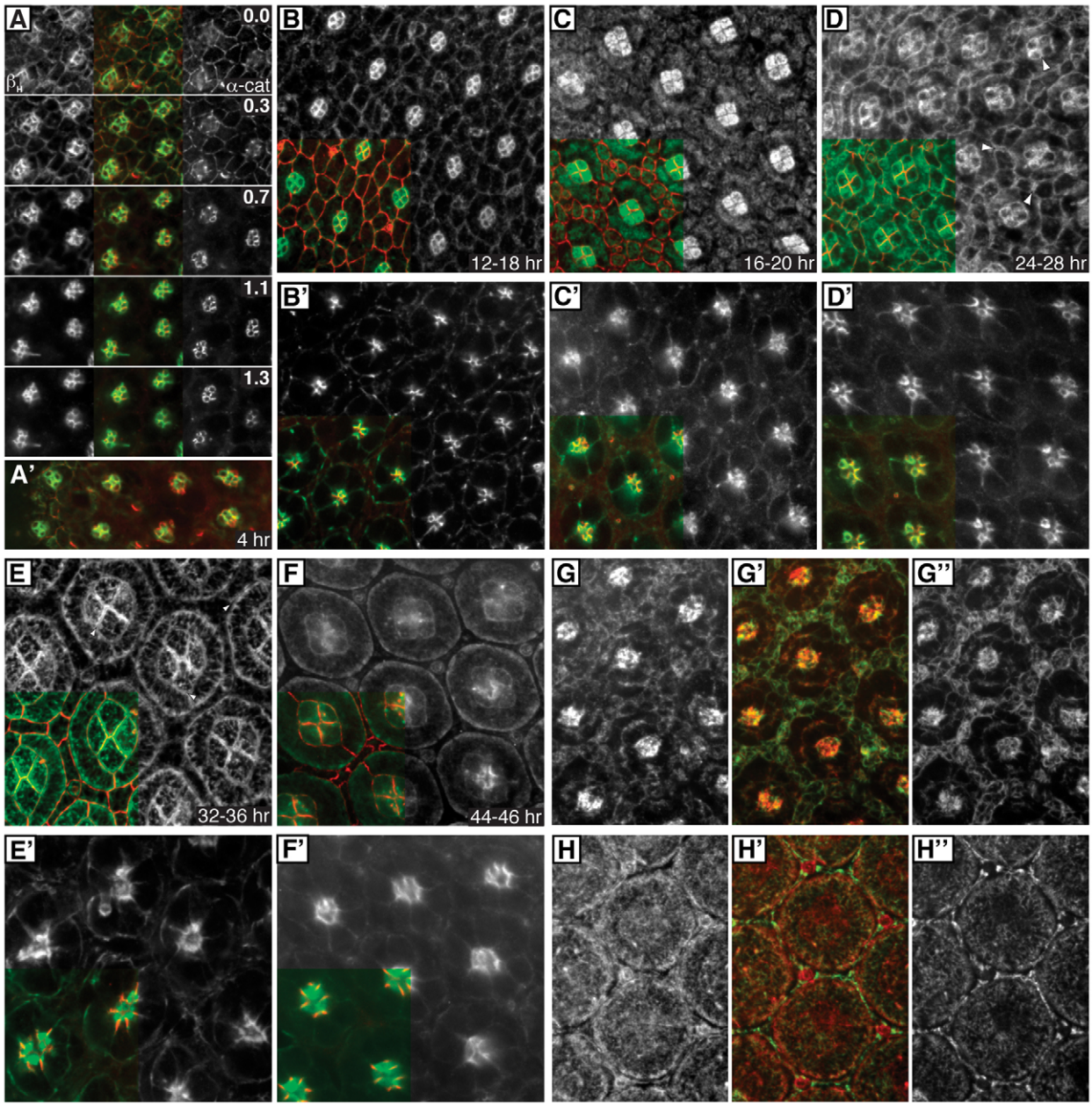

Fig. 4. The distribution of β_H during wild-type eye development. (**A-F′**) Immunolocalization of β_H in wild-type discs expressing α-catenin::GFP. All false color images are shown with α-catenin in red and β_H in green. (A) Images from a confocal Z-series taken of a 4- to 5-hour disc just when the photoreceptors are leaving the surface and reorienting their apical membranes towards each other. Numbers indicate the distance (in μm) below the '0.0' panel. Left column, β_H; right column, α-catenin; center column, merged image. Apical contacts are still present between the cone cells and photoreceptors at this stage. β_H is diffusely present on the apical surface (0.0) and colocalizes with the ZA below. Some areas of α-catenin signal without apparent β_H colocalization are visible. This is particularly evident in A′, which shows a single confocal slice through a curved region of a disc so that the image proceeds from apical (left) to basal (right). Note that there are some regions where β_H does not colocalize with α-catenin. (B-F) β_H staining at the level of the ZA. (B′-F′) Immunolocalization of β_H in wild-type discs at the level of the photoreceptor cells. Insets in B-F and B′-F′ are contiguous with the main panel and show colocalization of β_H (green) and α-catenin (red). β_H colocalizes with α-catenin until cell migration is completed (12-18 hours), whereupon β_H becomes apical or sub-cortical and distinct from α-catenin. (**G-H″**) Immunolabeling of β_H (G,H, shown in red in merged images G′and H′) in wild-type discs expressing GFP-moesin as a marker for F-actin (G″,H″, shown in green in merged images). Apart from some differences in signal intensity in some cell types, both proteins show very similar, but non-identical distributions (see text for discussion).

is once more seen near the ZA region after the IOC ZAs are re-established and the secondary cells begin to narrow (Fig. 4D). At this stage the distributions of β_H in neighboring cells show obvious separations indicating a distribution subcortical to the ZA (Fig. 4D; arrowheads). At around 32-36 hours the distribution again undergoes a dramatic change and β_H is again prominent across the apical surface in a planar, distinctly fibrous distribution (Fig. 4E). This is most obvious in the cone and primary cells and is conspicuously radial in the latter (Fig. 4E), and again appears to terminate in the subcortical region of the ZA. As the IOCs continue to narrow, β_H

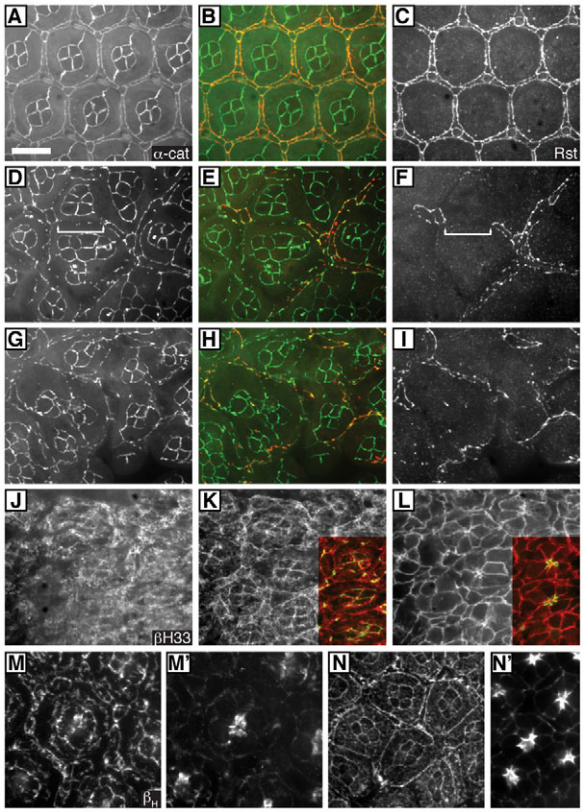

Fig. 5. Disruption of the ZA is accompanied by loss of Roughest staining. Expression of Roughest (shown by immunofluorescence) along with α-catenin::GFP in pupal discs. (**A-C**) Wild-type disc showing how Roughest labeling is confined to the primary cell-IOC boundary and some conspicuous internal compartments at this stage (~44 hours). (**D-I**) Two examples of similarly staged GMR>βH33-expressing discs, showing that fragmentation of the ZA is associated with loss of Roughest staining (brackets in D and F indicate an example). This result is consistent with the previously reported dependency of Roughest on the integrity of the ZA. (**J-L**) Staining for βH33 in the developing GMR>βH33 retina. βH33 is localized on all plasma membrane surfaces. Color overlays in K and L show colocalization with α-catenin::GFP. (**M-N′**) Distribution of β_H in GMR>βH33 retina. (M,M′) an ~24- to 28-hour disc (slightly higher magnification); (N,N′) an ~36- to 46-hour disc. β_H is not displaced from the membrane by βH33 and developmental changes described in Fig. 4A-F are still discernable despite the tissue disruption (compare M, M′ with Fig. 4E-F′ and N, N′ with Fig. 4D,D′). The antibody used (#243) does not recognize βH33. Scale bar: 10 μm.

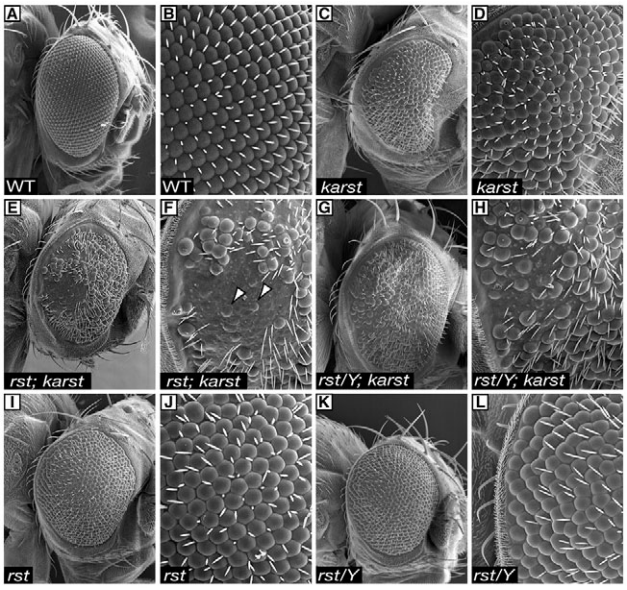

Fig. 6. Genetic interaction between *karst* and *rst*. Scanning electron micrographs of adult eyes. (**A**,**B**) Wild-type eye. (**C**,**D**) *karst* mutant eyes have a slight roughness and occasional flat spots with no lens. Note that these are siblings from the interaction test cross with the genotype *Fm7/Y; $kst^{14.1}/kst^{RH445}$* and that the kidney-shape of the eye arises from the dominant marker *Bar* on the Fm7 chromosome. This is irrelevant to this analysis. (**E**,**F**) Eye from female homozygous for both *rst* and *karst* (*rst^{CT}; $kst^{14.1}/kst^{RH445}$*). Large numbers of ommatidia drop down (arrowheads) or are entirely invisible from surface morphology. (**G**,**H**) Eye from male hemizygous for *rst* and homozygous for *karst* (*rst^{CT}/Y, $kst^{14.1}/kst^{RH445}$*). Again many ommatidia fall from the retinal surface, although this is less pronounced than in the females. (**I**,**J**) Eye from female homozygous for *rst* (*rst^{CT}*). Mild roughening is evident. (**K**,**L**) Eye from male hemizygous for *rst* (*rst^{CT}/Y*). Mild roughening is evident. Some ommatidia fall all the way to the optic lobe (see supplementary material Fig. S3 for sections of some of these genotypes).

remains prominent at the apical surface in the cone and primary cells. However, it is now present in a more uniform, hazy distribution that is concentrated in the primary cells at the IOC boundary, and in the cone cells at the ZA. Although most of the IOCs have a relatively low level of β_H at the later stages, it is more prominent in the bristle and socket cells.

The dynamic patterns of β_H accumulation are strikingly similar to the distribution of F-actin (Johnson et al., 2008). Optimal fixation for β_H requires the use of methanol, precluding colocalization studies with fluorescent phalloidin. We therefore used the GFP-tagged moesin actin-binding domain as a reporter for F-actin (Edwards et al., 1997). Using this reporter β_H has a very similar, but not identical pattern of staining (Fig. 4G-H). This might reflect a genuine difference in localization or a perturbation induced by methanol treatment or GFP-moesin binding. In either case β_H dynamics appear to be closely associated with rearrangements in the bulk F-actin cytoskeleton. In summary, these results indicate that β_H colocalizes with the ZA during IOC morphogenesis and is subsequently more loosely associated with this structure, exhibiting striking accumulations resembling F-actin at later stages of development.

βH33 expression disrupts the distribution of Roughest and the ZA, but not β_H

IOC morphogenesis is mediated by Roughest (Araujo et al., 2003; Reiter et al., 1996). We therefore stained GMR>βH33 + α-catenin::GFP pupal eye discs for Roughest. During IOC morphogenesis Roughest is normally present at the IOC-primary cell boundary, as well as in some internal vesicular structures (Fig. 5A-C). In GMR>βH33 discs, the ZA are fragmented and Roughest is conspicuously absent at these locations. This is consistent with previous observations that the distribution of Roughest is dependent on the integrity of the ZA (Fig. 5D-I) (Grzeschik and Knust, 2005) and vice versa (Bao and Cagan, 2005).

We next localized βH33 and β_H in GMR>βH33 flies via its Myc tag (Williams et al., 2004). βH33 exhibits an unpolarized membrane distribution at all stages in all cell types (Fig. 5J-L). Staining for β_H in GMR>βH33 flies reveals a distribution that is essentially unperturbed (Fig. 5M,N). This observation suggests that βH33 does not simply displace β_H from the membrane, but is probably targeting a specific β_H interaction. These results are very similar to

those seen when βH33 is expressed in the embryonic salivary gland (Williams et al., 2004). They also indicate that cortical localization of β_H is not dependent upon either the ZA or Roughest.

Genetic interaction between *karst* and *rst*

We next checked for a genetic interaction between loss-of-function *karst* (*kst*) and *roughest* (*rst*) alleles. *rst/Y* males and *rst* homozygous females exhibit a mild roughening of the adult eye because IOC movement does not occur properly and too many cells survive, resulting in an excess of secondary and tertiary pigment cells (Araujo et al., 2003; Reiter et al., 1996; Fig. 6I-L). In flies that are also heterozygous for $kst^{14.1}$ (*rst/Y;* $kst^{14.1}$/+), this roughness is slightly more pronounced with more 'fused' lenses (an indicator of IOC loss; not shown). When we tried to make doubly homozygous *rst; kst* combinations using the strong loss-of-function combination ($kst^{14.1}$/*Df(3L)1226*) no adult flies developed suggesting that *karst* lethality is enhanced by *rst*. However, we were able to obtain *rst/Y* males in combination with the milder $kst^{14.1}/kst^{RH445}$ combination (kst^{RH445} is an hypomorphic P-element insertion in the β_H 5′-UTR that produces reduced amounts of full-length protein; E. M. Morariu and C.M.T., unpublished results). In this combination, there is a conspicuous enhancement of the *karst* phenotype (Fig. 6C,D) caused by the reduction in Roughest (Fig. 6E-H). This is characterized by a severe loss of inter-cluster adhesion with whole ommatidia dropping down (arrowheads in supplementary material Fig. S3B), or completely falling out of the retina into the optic lobe, a characteristic also of *karst* mutant eyes (arrowhead; supplementary material Fig. S3A). This descent appears selective because all of the pigment granules in this region are small and closely associated with rhabdomeres in photoreceptors, indicating that no pigment cells are seen within the optic lobe (inset; supplementary material Fig. S3B). Conspicuously more ommatidia are seen in this region in the *rst*; *karst* combinations (supplementary material Fig. S3C). In addition, secreted lens material is seen within the retina (not shown) indicating that cone and primary cells [which secrete the lens (Wolff and Ready, 1993)] are also falling from the surface. This suggests that the failure in adhesion is occurring at the IOC-primary cell boundary, which is the site of Roughest protein accumulation during IOC morphogenesis. These data indicate that heterozygous *karst* mutations enhance *rst*, and that in homozygous combination the *karst* and *rst* mutations have a strong synergistic effect indicative of a close functional relationship.

Physical interaction between β_H and Roughest

One mechanism by which Roughest might be stabilized at the plasma membrane by β_H is through a direct or indirect physical association. Roughest is a member of the immunoglobulin superfamily of cell adhesion molecules (Ig-CAM). The L1 subset of this superfamily interacts with conventional β-spectrin via the adaptor protein Ankyrin (Herron et al., 2009; Hortsch et al., 2009). However, neither Roughest nor β_H contains a recognizable Ankyrin binding site (Strunkelnberg et al., 2003; Thomas et al., 1997). Moreover, β_H does not colocalize with Ankyrin by immunofluorescence (Dubreuil et al., 1997). However, there remains the possibility of a β_H-Roughest interaction mediated via another mechanism. β_H is only visibly colocalized with Roughest during early pupal development. At this stage pupal disc dissection is at its most difficult and histolysis of larval tissues is at its peak, two factors making coimmunoprecipitation of this labile protein (Vishnu et al., 2006) from pupal discs extremely challenging. We therefore chose to search for this interaction during embryonic development where the two proteins have nearly identical distributions in the ectodermal epithelium and musculature (supplementary material Fig. S4). As shown in Fig. 7A, Roughest is indeed specifically brought down from embryonic extracts in a β_H immune complex, indicative of a direct or indirect physical interaction between these two proteins.

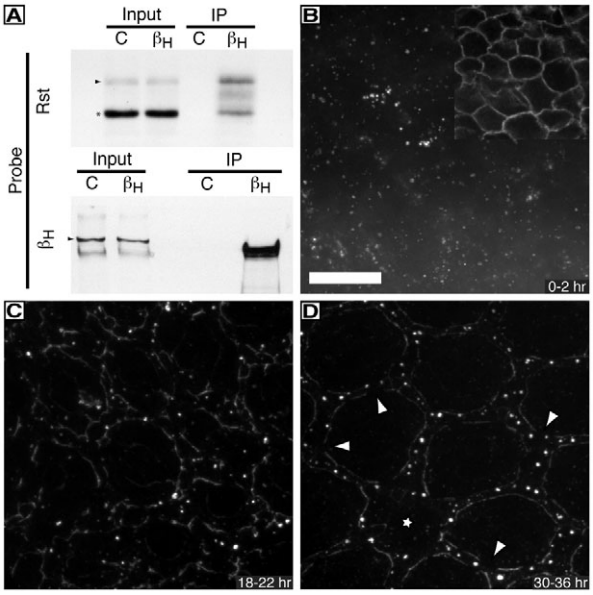

Fig. 7. Physical interaction between β_H and Roughest. (**A**) Immunoprecipitation experiment using embryonic extracts and either affinity purified anti-β_H antibodies (β_H) or an anti-Fasciclin III control (C). Blots were then probed for either Roughest (top) or β_H (bottom). Roughest is found specifically in immunoprecipitates (IP) with β_H. In our hands, as with others (Vishnu et al., 2006), Roughest is extremely labile and a prominent breakdown product (asterisk) is visible along with the full-length protein (arrowhead). As a consequence our 'input' samples were taken at the end of the incubation (3% of supernatant) to demonstrate that some full-length Roughest survives. (**B-D**) Staining for Roughest protein in kst^{2}/*Df(3L)1226* pupal eye discs. Roughest is not localized to the membrane at early stages of development but is prominent in intracellular vesicular structures (B). Inset: co-staining for α-spectrin in the lateral membrane to show cell boundaries [α-spectrin is lost from the apical membrane in *karst* mutants (Zarnescu and Thomas, 1999)]. At later stages (C,D) when Roughest normally accumulates prominently at the IOC-primary cell boundary (e.g. Fig. 5C), lower than normal membrane localization is seen with many conspicuous gaps (arrowheads). The star indicates the loss of an ommatidium (see Fig. 6). Main images are maximum projections of several confocal sections as Roughest puncta are distributed along the apicobasal axis. Scale bar: 10 μm.

Physical association of transmembrane proteins with the spectrin cytoskeleton has been correlated with stabilization of proteins at the cell surface (reviewed by Bennett and Baines, 2001; De Matteis and Morrow, 2000). We therefore performed immunostaining for Roughest in *karst* mutant discs. In wild-type eye discs, Roughest is distributed both in a dynamic sequence of locations at the membrane, as well as in numerous cytoplasmic puncta in an unidentified compartment (Ramos et al., 1993). In *karst* mutant eyes we see only Roughest-positive puncta at early stages of pupal eye development (Fig. 7B) and weak, interrupted stretches of membrane staining at later stages (Fig. 7C,D). This indicates that wild-type Roughest localization at the plasma membrane depends on an intact apical spectrin membrane skeleton in the eye, and is consistent with a physical and functional association between the two proteins in this tissue.

Discussion

Our investigation of the overexpression of β_H segment 33 (βH33) in the eye disc has shown that the phenotype it induces is closely associated with a morphogenetic event that is required for a normal round of apoptosis that refines the retinal lattice. This disruption is correlated with disruption of the ZA and the normal distribution of the Roughest protein, which mediates this morphogenesis. Further experiments demonstrated a strong genetic interaction between loss-of-function *karst* and *rst* alleles that appears to result in reduced adhesion between IOCs and ommatidia. Finally, we demonstrate, by coimmunoprecipitation a physical association between β_H and the Roughest protein, and that the distribution of Roughest is significantly disrupted in *karst* mutant cells.

As part of a genetic study to probe the function of the β_H C-terminal domain (βH33), we took an overexpression approach to generate a dominant phenotype (see Herskowitz, 1987). We have found that the overexpression of this domain disrupts development, is associated with acridine orange accumulation and can be ameliorated by coexpression of the baculovirus p35 caspase inhibitor, revealing it to be at least in part apoptotic (Williams et al., 2004). This is a specific effect of the apical β_H isoform, because overexpression of the C-terminus of the related basolateral β-spectrin produces no such phenotype (Williams et al., 2004).

βH33 contains a PH domain, which is required to induce this phenotype (Williams et al., 2004), indicating a requirement for lipid binding or overlapping protein binding (e.g. Touhara et al., 1995). Sequestration of phospholipids is an obvious possible cause of the βH33-induced phenotype and in particular apoptosis. As a class, β-spectrin PH domains appear to use phosphatidylinositol 4,5-bisphosphate [PtdIns(4,5)P_2] binding as a major mechanism for membrane association (Das et al., 2008; Hyvonen et al., 1995; Lombardo et al., 1994; Zhang et al., 1995). Furthermore, modulation of PtdIns(4,5)P_2 levels regulates spectrin association with the Golgi membrane (Godi et al., 1998; Siddhanta et al., 2003) and secretory vesicles (Muresan et al., 2001). We demonstrate here that the β-spectrin and β_H PH domain regions have nearly identical phospholipid specificities, and that they both exhibit the distinct preference for PtdIns(4,5)P_2 over PtdIns(3,4,5)P_3 seen by Das et al. (Das et al., 2008) for β-spectrin. The only difference is a conspicuous affinity of β-spectrin for phosphatidic acid that is not detectable with β_H. This difference probably arises from a second lipid-binding site outside the PH domain, and does not readily account for the lack of phenotype during β-spectrin PH domain expression. The requirement for phospholipid binding in this case might therefore represent only a membrane anchoring mechanism for the ectopic βH33 domain. Finally, these results strongly indicate that bulk differences in phospholipid content are unlikely to be a driving force in the apical-basal polarization of β_H and β-spectrin in *Drosophila*.

Integration of cell adhesion systems

In the fly eye, a round of apoptosis during pupation eliminates excess IOCs to refine the retinal epithelium. During this period IOCs compete for contact with the primary cells and rearrange into a single row of pigment and bristle cells surrounding each ommatidium, whereas apoptosis culls their numbers to produce an almost crystalline lattice. IOC morphogenesis is mediated by Roughest, which is expressed only in the IOCs at this time where it binds to Hibris expressed on the surface of neighboring primary cells (Bao and Cagan, 2005). Roughest colocalizes with the cadherin-based ZA and is both dependent upon the ZA (Grzeschik and Knust, 2005) and in turn modulates the properties of the ZA (Bao and Cagan, 2005). Our results tighten the association between these two adhesion systems, providing a potential common mediator for their activities.

During eye development β_H is recruited to the membrane by a domain in the Crumbs protein (Pellikka et al., 2002), which specifically regulates ZA stability but not polarity (Klebes and Knust, 2000; Medina et al., 2002). As a consequence, mutants that lack wild-type β_H exhibit a mild and variable disruption of the ZA, but maintain normal apicobasal polarity (Zarnescu and Thomas, 1999). We show here that β_H also has a physical association with Roughest during embryonic development; however, it is not yet possible to say whether this is via direct binding or is an indirect association via another protein, as with Crumbs (Klebes and Knust, 2000; Medina et al., 2002). Physical association with spectrin can result in protein stabilization at the plasma membrane, and so the disruption of Roughest distribution in *karst* mutant discs strongly suggests that this physical association holds true in the eye. Thus, we propose that Crumbs-driven assembly of the apical spectrin-based membrane skeleton provides a means to coordinate the ZA and Roughest/Hibris adhesion systems. If binding of Roughest to β_H mediates this coordination at the plasma membrane it must presumably occur when β_H is at the ZA before or during cell movement.

Emerging data suggest a role for β_H in protein trafficking: β_H co-isolates with the Golgi-resident protein Lava lamp (Sisson et al., 2000), and a dramatic reduction in the surface expression level of the apical V-type H^+-ATPase in the gut is seen when β_H-dependent protein recycling is disrupted in *karst* mutants (Phillips and Thomas, 2006). It is therefore possible that β_H could play a similar role for Roughest in the eye. The increased levels of Roughest protein in cytoplasmic puncta in *karst* mutant discs are consistent with this notion. In this context, it is interesting to note that deletion of the Roughest cytoplasmic domain in the rst^{CT} allele (Ramos et al., 1993), which would be predicted to uncouple it from β_H, also leads to elevated levels of vesicular Roughest protein (Reiter et al., 1996). Because Rst^{CT} protein is unlikely to have any residual association with β_H, we suggest that the strong synergism of the rst^{CT}-*karst* interaction arises from the simultaneous reduction of Roughest and ZA function below a threshold where adhesion is insufficient for IOC-primary cell adhesion.

βH33 and *karst* both disrupt Roughest distribution, but with different consequences: βH33 primarily affects IOC, whereas *karst* causes selective falling of ommatidia from the retina. We speculate that the prominent accumulation of Roughest and β_H at the IOC-primary cell boundary late in development is necessary to hold the ommatidia in place. Thus, simultaneous reduction in the function of both proteins selectively weakens this interface. By contrast, βH33 would appear to be having its effect earlier during morphogenesis. Given the lack of an obvious direct stimulation of any apoptotic pathway by βH33 expression, coupled with the novel association of β_H with Roughest and its known role in cell survival decisions, we suggest that the apoptotic effects of this domain are an indirect result of the disruption of apicolateral cell junctions that in turn regulate cell survival. We speculate that the preferential loss of IOCs upon βH33 expression arises because the cell death or survival decisions that are made at this time arise from small differences in cell adhesion in amongst the IOCs that are 'predisposed' to die if a lower threshold is reached: reducing junction function at this time thus greatly, and selectively, increases the number of IOCs that die.

Spectrin and Ig-CAMs

Conventional β-spectrins are well known to associate with Ig-CAMs of the L1 subfamily via the adapter molecule Ankyrin (Herron et al., 2009; Hortsch et al., 2009). Roughest belongs to a different subfamily that includes Nephrin and has a completely divergent cytoplasmic domain that lacks the conventional Ankryin binding site (Strunkelnberg et al., 2003). Similarly, β_H lacks the canonical Ankyrin binding domain (Thomas et al., 1997) and does not colocalize with Ankyrin in vivo (Dubreuil et al., 1997). This raises an interesting evolutionary question as to whether a proto-spectrin was bound to a common proto-Ig-CAM and that divergence of the spectrins and Ig-CAMs was accompanied by the acquisition or loss of Ankyrin as an adaptor in the conventional or heavy β-spectrin lineage, or whether the spectrin–Ig-CAM association came later and this is an example of convergence. Because all of these proteins appear to have emerged at around the time that multicellular animals evolved, we cannot readily answer this at present. Moreover, the separation of conventional and heavy β-spectrins occurred during a period of dynamic concerted evolution that might have erased the evidence within the spectrins themselves (Thomas et al., 1997). It will be interesting to see if the β_H–Ig-CAM association extends to other members of this subfamily such as Hibris, the Roughest ligand.

Materials and Methods

Fly stocks

Flies were maintained on standard cornmeal-agar food with all crosses carried out at defined temperatures to standardize GAL4 expression levels. The generation of the line *P{w*$^{+mc}$ *kst*$^{\beta H33.Scer\UAS.T:Hsap\MYC}$=*βH33}*, which expresses β_H segment 33 has been previously described (Williams et al., 2004). The lines *P{69B-GAL4}* and *rst*^{CT} were obtained from the Bloomington Drosophila Stock Center (Bloomington, IN). The *P{eyeless-GAL4}* line was obtained from Andreas Wodarz (Georg-August-Universität Göttingen, Göttingen, Germany). The *P{GMR-p35}* line (Hay et al., 1994) was obtained from Gerald Rubin (HHMI Janelia Farm Research Campus, Ashburn, VA). *P{GMR-GAL4}* (Golembo et al., 1996) was obtained from Zhi-Chun Lai (Penn State, University Park, PA). *P{UAS-PLCγPH::GFP}* was obtained from Lynn Cooley (Yale School of Medicine, New Haven, CT). The *P{hs-cycA}* line was obtained from Tin Tin Su (University of Colorado, Boulder, CO). *P{UAS-α-catenin::GFP}* was obtained from Hiroki Oda (JT Biohistory Research Hall, Osaka, Japan). The *P{UAS-Moe::GFP}* line (Edwards et al., 1997) was obtained from Daniel P. Kiehart (Duke University, Durham, NC).

FACS analysis of cell cycle phase in imaginal discs

Eye-antennal and wing imaginal discs from late third instar larvae were dissected in *Drosophila* Ringer's solution (Ashburner, 1989), washed once in Ringer's solution, then transferred to 130 µl extraction buffer (60 mM KCl, 15 mM NaCl, 1 mM EDTA, 0.1 mM EGTA, 15 mM Tris-HCl pH 7.4, 0.15 mM spermine, 0.5 mM spermidine, 0.5 mM DTT) (Hewish and Burgoyne, 1973) on ice. Tissue was homogenized in a 1.5 ml Eppendorf tube using a motorized micropestle for ~2 minutes and brought to 500 µl with a further 370 µl of extraction buffer that also served as a wash to recover any material remaining on the pestle. 0.5 µl Syto16 dye (Molecular Probes) was added and the sample incubated on ice for at least 30 minutes to facilitate dye uptake. Nuclei were counted and DNA content estimated without further purification on an XL-MCL flow cytometer (Beckman-Coulter) using a 488 nm argon laser for excitation. Dual multiparameter analysis of peak height and integral fluorescence was performed to eliminate fluorescence due to cellular debris and doublets. Histograms collected on multiparameter gated cells (10,000 events) were analyzed using Multicycle DNA cell cycle analysis software Autofit (v 2.53; Phoenix Flow Systems, San Diego, CA). As a positive control, cells were driven into S-G2 phase by overexpression of cyclin A (Lehner et al., 1991). Third instar larvae carrying the *P{hs-cycA}* transgene were heat-shocked at 37°C for 1 hour and allowed to recover for 1 hour at room temperature, before dissection and FACS analysis as described above.

Antibodies

Polyclonal rabbit anti-β_H (#243) was used for immunofluorescence (1:100) and in affinity purified form for immunoprecipitation and in some late-stage immunofluorescence experiments (1:10). Monoclonal anti-Fasciclin III (#7G10; 1:10) developed by C. Goodman was obtained from the Developmental Studies Hybridoma Bank developed under the auspices of the NICHD and maintained by The University of Iowa, Department of Biology, Iowa City, IA 52242. Monoclonal anti-Roughest antibodies (#21D11 for immunoblots and #24A5.1 for immunofluorescence; both 1:10) were obtained from Karl-Friedrich Fischbach (University of Freiburg, Freiburg, Germany). Rabbit anti-phosphohistone H3 antibody (1:100) was obtained from Upstate Biotechnology. Monoclonal anti-Myc (#9E10; 1:100) was obtained from Calbiochem. Alexa-Fluor-conjugated secondary antibodies (1:250) were obtained from Molecular Probes.

Immunofluorescent staining and imaging

For timing purposes, pupae were selected as white prepupae and maintained at 25°C for the times indicated in figures. Eye-antennal imaginal discs and pupal eye discs were dissected, fixed in 4% w/v paraformaldehyde in PEM (0.1 M PIPES pH 6.5, 1 mM $MgCl_2$, 1 mM EGTA), washed twice with PBS and post-fixed in 100% methanol for 10 minutes. Following rehydration through a decreasing methanol series, the fixed tissue was extracted in with PB5T (PBS, 0.5% Triton X-100) and blocked with 10% normal goat serum (NGS) in PBSTD (PBS, 0.2% saponin, 0.3% Triton X-100, 0.3% deoxycholate) (Bao and Cagan, 2005) for 1 hour. All subsequent incubations were done in PB5T supplemented with 5% NGS. Primary and secondary antibody incubations were done at 4°C for a minimum of 12 hours. Specimens were imaged using a BD Biosciences Carv II spinning disc confocal imager mounted on an Olympus BX50 microscope (Olympus America, Lake Success, NY). For microscope control, image acquisition and post processing iVision software (BioVision Technologies, Exton, PA) was used.

Immunoprecipitation and immunoblotting

The 0-24 hour embryos were dechorionated in 50% bleach, rinsed in 0.1% Triton X-100 and twice in cold extraction buffer (50 mM Tris-HCl pH 8.5, 150 mM NaCl, 0.5% sodium deoxycholate) supplemented with protease inhibitors (50 µg/ml PMSF, 1 µg/ml leupeptin, 1.4 µg/ml pepstatin, 50 µg/ml benzamidine; Boehringer Mannheim) and phosphatase inhibitors (1 mM NaF, 400 µM $NaVO_3$, 400 µM $NaVO_4$; Sigma-Aldrich). A ~300 µl settled volume of embryos was disrupted in 10 volumes of extraction buffer using 10-20 strokes in a Dounce homogenizer. After clarification at 17,000 ***g***, aliquots were incubated with either affinity purified anti-β_H antibody or anti-Fasciclin III as a control for 2 hours a 4°C. Immune complexes were recovered using protein-A-Sepharose beads (40 µl settled volume/ml sample; Sigma-Aldrich) that were prepared according to the manufacturer's instructions and pre-washed with extraction buffer. Beads were recovered by brief centrifugation and washed several times with extraction buffer, resuspended directly in loading buffer and boiled to elute.

Eye sectioning and scanning electron microscopy

Fly heads were fixed and sectioned using standard methodologies (Tomlinson, 1985). Scanning electron microscopy was carried out as described previously (Thomas et al., 1998) and imaged using a Joel model JSM5400 scanning electron microscope.

Phospholipid binding assays

To assay phospholipid binding by the PH domain regions of β_H and β-spectrin, the regions expressed from the βHPH+3 and βspPH transgenes (Williams et al., 2004) were recloned into the appropriate pGEX vector. Expression of just the PH domain (region ii in Fig. 1) fused to GST was not possible in bacteria and could not be achieved from a transgene in flies either. Thus we fused codons 3747-3920 of β_H to GST. This covers regions ii and iii of segment 33 from β_H (Fig. 1). To best match the regions tested from the two spectrins, βspPH contained codons 2131-2291 of β-spectrin, which similarly stretches from the N-terminal end of the PH domain for about the same distance to the natural C-terminus of this protein. Both fusion proteins were induced, extracted and purified using glutathione-Sepharose 4B (Amersham Biosciences, Piscataway, NJ) according to the manufacturer's instructions. Phospholipid specificity was assayed using PIP strips (Echelon Biosciences, Salt Lake City, UT). The fusion proteins were applied to the strips at 500 ng/ml, with blocking, incubation and subsequent processing according to the manufacturer's instructions at pH 7.5. To detect bound protein we used HRP-conjugated anti-GST antibody at 1:2000 and ECL developing reagents (Amersham Biosciences).

We would like to thank the many investigators (see Materials and Methods) as well the Bloomington Drosophila Stock Center for supplying fly stocks and antibodies. We also thank Elaine Kunze for assistance with flow cytometry, Maura Strauss, Rosemary Walsh, Michelle Pfieffer and Missy Hazen for assistance with electron microscopy, as well as Randen Patterson and Enkelejda Bashllari for assistance with the PIPStrips. Finally we thank Esther Siegfried and members of the Thomas laboratory for critically reading this manuscript. This work was supported by a National Science Foundation grant (#0644691) to C.M.T.

Supplementary material available online at
http://jcs.biologists.org/cgi/content/full/123/2/277/DC1

References

Araujo, H., Machado, L. C., Octacilio-Silva, S., Mizutani, C. M., Silva, M. J. and Ramos, R. G. (2003). Requirement of the roughest gene for differentiation and time of death of interommatidial cells during pupal stages of Drosophila compound eye development. *Mech Dev.* **120**, 537-547.

Ashburner, M. (1989). *Drosophila; A Laboratory Handbook*. Cold Spring Harbor, NY: Cold Spring Harbor Press.
Assemat, E., Bazellieres, E., Pallesi-Pocachard, E., Le Bivic, A. and Massey-Harroche, D. (2008). Polarity complex proteins. *Biochim. Biophys. Acta* **1778**, 614-630.
Baker, N. E. and Yu, S. Y. (2001). The EGF receptor defines domains of cell cycle progression and survival to regulate cell number in the developing Drosophila eye. *Cell* **104**, 699-708.
Bao, S. and Cagan, R. (2005). Preferential adhesion mediated by Hibris and Roughest regulates morphogenesis and patterning in the Drosophila eye. *Dev. Cell* **8**, 925-935.
Bennett, V. and Baines, A. J. (2001). Spectrin and ankyrin-based pathways: metazoan inventions for integrating cells into tissues. *Physiol. Rev.* **81**, 1353-1392.
Brazil, D. P. and Hemmings, B. A. (2001). Ten years of protein kinase B signalling: a hard Akt to follow. *Trends Biochem. Sci.* **26**, 657-664.
Cabodi, S., Moro, L., Bergatto, E., Boeri Erba, E., Di Stefano, P., Turco, E., Tarone, G. and Defilippi, P. (2004). Integrin regulation of epidermal growth factor (EGF) receptor and of EGF-dependent responses. *Biochem. Soc. Trans.* **32**, 438-442.
Carthew, R. W. (2007). Pattern formation in the Drosophila eye. *Curr. Opin. Genet. Dev.* **17**, 309-313.
Das, A., Base, C., Manna, D., Cho, W. and Dubreuil, R. R. (2008). Unexpected complexity in the mechanisms that target assembly of the spectrin cytoskeleton. *J. Biol. Chem.* **283**, 12643-12653.
De Matteis, M. A. and Morrow, J. S. (2000). Spectrin tethers and mesh in the biosynthetic pathway. *J. Cell Sci.* **113**, 2331-2343.
Dubreuil, R. R., Maddux, P. B., Grushko, T. A. and MacVicar, G. R. (1997). Segregation of two spectrin isoforms: polarized membrane-binding sites direct polarized membrane skeleton assembly. *Mol. Biol. Cell* **8**, 1933-1942.
Edwards, K. A., Demsky, M., Montague, R. A., Weymouth, N. and Kiehart, D. P. (1997). GFP-moesin illuminates actin cytoskeleton dynamics in living tissue and demonstrates cell shape changes during morphogenesis in Drosophila. *Dev. Biol.* **191**, 103-117.
Ferguson, K. M., Kavran, J. M., Sankaran, V. G., Fournier, E., Isakoff, S. J., Skolnik, E. Y. and Lemmon, M. A. (2000). Structural basis for discrimination of 3-phosphoinositides by pleckstrin homology domains. *Mol. Cell* **6**, 373-384.
Godi, A., Santone, I., Pertile, P., Devarajan, P., Stabach, P. R., Morrow, J. S., Di Tullio, G., Polishchuk, R., Petrucci, T. C., Luini, A. et al. (1998). ADP ribosylation factor regulates spectrin binding to the Golgi complex. *Proc. Natl. Acad. Sci. USA* **95**, 8607-8612.
Golembo, M., Schweitzer, R., Freeman, M. and Shilo, B. Z. (1996). Argos transcription is induced by the *Drosophila* EGF receptor pathway to form an inhibitory feedback loop. *Development* **122**, 223-230.
Grawe, F., Wodarz, A., Lee, B., Knust, E. and Skaer, H. (1996). The *Drosophila* genes *crumbs* and *stardust* are involved in the biogenesis of adherens junctions. *Development* **122**, 951-959.
Grzeschik, N. A. and Knust, E. (2005). IrreC/rst-mediated cell sorting during *Drosophila* pupal eye development depends on proper localisation of DE-cadherin. *Development* **132**, 2035-2045.
Hay, B. A., Wolff, T. and Rubin, G. M. (1994). Expression of baculovirus P35 prevents cell death in *Drosophila*. *Development* **120**, 2121-2129.
Herron, L. R., Hill, M., Davey, F. and Gunn-Moore, F. J. (2009). The intracellular interactions of the L1 family of cell adhesion molecules. *Biochem. J.* **419**, 519-531.
Herskowitz, I. (1987). Functional inactivation of genes by dominant negative mutations. *Nature* **329**, 219-222.
Hewish, D. R. and Burgoyne, L. A. (1973). Chromatin sub-structure. The digestion of chromatin DNA at regularly spaced sites by a nuclear deoxyribonuclease. *Biochem. Biophys. Res. Comm.* **52**, 504-510.
Hollande, F., Shulkes, A. and Baldwin, G. S. (2005). Signaling the junctions in gut epithelium. *Sci. STKE* **2005**, pe13.
Hortsch, M., Nagaraj, K. and Godenschwege, T. A. (2009). The interaction between L1-type proteins and ankyrins-a master switch for L1-type CAM function. *Cell Mol. Biol. Lett.* **14**, 57-69.
Hyvonen, M., Macias, M. J., Nilges, M., Oschkinat, H., Saraste, M. and Wilmanns, M. (1995). Structure of the binding site for inositol phosphates in a PH domain. *EMBO J.* **14**, 4676-4685.
Johansson, M., Rocha, N., Zwart, W., Jordens, I., Janssen, L., Kuijl, C., Olkkonen, V. M. and Neefjes, J. (2007). Activation of endosomal dynein motors by stepwise assembly of Rab7-RILP-p150Glued, ORP1L, and the receptor betalll spectrin. *J. Cell Biol.* **176**, 459-471.
Johnson, R. I., Seppa, M. J. and Cagan, R. L. (2008). The Drosophila CD2AP/CIN85 orthologue Cindr regulates junctions and cytoskeleton dynamics during tissue patterning. *J. Cell Biol.* **180**, 1191-1204.
Kafer, J., Hayashi, T., Maree, A. F., Carthew, R. W. and Graner, F. (2007). Cell adhesion and cortex contractility determine cell patterning in the Drosophila retina. *Proc. Natl. Acad. Sci. USA* **104**, 18549-18554.
Kizhatil, K., Davis, J. Q., Davis, L., Hoffman, J., Hogan, B. L. and Bennett, V. (2007a). Ankyrin-G is a molecular partner of E-cadherin in epithelial cells and early embryos. *J. Biol. Chem.* **282**, 26552-26561.
Kizhatil, K., Yoon, W., Mohler, P. J., Davis, L. H., Hoffman, J. A. and Bennett, V. (2007b). Ankyrin-G and beta2-spectrin collaborate in biogenesis of lateral membrane of human bronchial epithelial cells. *J. Biol. Chem.* **282**, 2029-2037.
Klebes, A. and Knust, E. (2000). A conserved motif in Crumbs is required for E-cadherin localisation and zonula adherens formation in Drosophila. *Curr. Biol.* **10**, 76-85.
Lehner, C. F., Yakubovich, N. and O'Farrell, P. H. (1991). Exploring the role of Drosophila cyclin A in the regulation of S phase. *Cold Spring Harb. Symp. Quant. Biol.* **56**, 465-475.
Lietzke, S. E., Bose, S., Cronin, T., Klarlund, J., Chawla, A., Czech, M. P. and Lambright, D. G. (2000). Structural basis of 3-phosphoinositide recognition by pleckstrin homology domains. *Mol. Cell* **6**, 385-394.
Lombardo, C. R., Weed, S. A., Kennedy, S. P., Forget, B. G. and Morrow, J. S. (1994). βII-spectrin (fodrin) and βIΣ2-spectrin (muscle) contain NH_2- and COOH-terminal membrane association domains (MAD1 and MAD2). *J. Biol. Chem.* **269**, 29212-29219.
Martin-Belmonte, F., Gassama, A., Datta, A., Yu, W., Rescher, U., Gerke, V. and Mostov, K. (2007). PTEN-mediated apical segregation of phosphoinositides controls epithelial morphogenesis through Cdc42. *Cell* **128**, 383-397.
Medina, E., Williams, J., Klipfell, E., Zarnescu, D., Thomas, C. and Le Bivic, A. (2002). Crumbs interacts with moesin and beta(Heavy)-spectrin in the apical membrane skeleton of Drosophila. *J. Cell Biol.* **158**, 941-951.
Muresan, V., Stankewich, M. C., Steffen, W., Morrow, J. S., Holzbaur, E. L. and Schnapp, B. J. (2001). Dynactin-dependent, dynein-driven vesicle transport in the absence of membrane proteins: a role for spectrin and acidic phospholipids. *Mol. Cell* **7**, 173-183.
Pellikka, M., Tanentzapf, G., Pinto, M., Smith, C., McGlade, C. J., Ready, D. F. and Tepass, U. (2002). Crumbs, the Drosophila homologue of human CRB1/RP12, is essential for photoreceptor morphogenesis. *Nature* **416**, 143-149.
Phillips, M. D. and Thomas, C. M. (2006). Brush border spectrin is required for early endosome recycling in *Drosophila*. *J. Cell Sci.* **119**, 1361-1370.
Ramos, R. G., Igloi, G. L., Lichte, B., Baumann, U., Maier, D., Schneider, T., Brandstatter, J. H., Frohlich, A. and Fischbach, K. F. (1993). The irregular chiasm C-roughest locus of Drosophila, which affects axonal projections and programmed cell death, encodes a novel immunoglobulin-like protein. *Genes Dev.* **7**, 2533-2547.
Reiter, C., Schimansky, T., Nie, Z. and Fischbach, K. F. (1996). Reorganization of membrane contacts prior to apoptosis in the *Drosophila* retina: the role of the IrreC-rst protein. *Development* **122**, 1931-1940.
Scanga, S. E., Ruel, L., Binari, R. C., Snow, B., Stambolic, V., Bouchard, D., Peters, M., Calvieri, B., Mak, T. W., Woodgett, J. R. et al. (2000). The conserved PI3′K/PTEN/Akt signaling pathway regulates both cell size and survival in Drosophila. *Oncogene* **19**, 3971-3977.
Siddhanta, A., Radulescu, A., Stankewich, M. C., Morrow, J. S. and Shields, D. (2003). Fragmentation of the Golgi apparatus. A role for beta III spectrin and synthesis of phosphatidylinositol 4,5-bisphosphate. *J. Biol. Chem.* **278**, 1957-1965.
Sisson, J. C., Field, C., Ventura, R., Royou, A. and Sullivan, W. (2000). Lava lamp, a novel peripheral golgi protein, is required for Drosophila melanogaster cellularization. *J. Cell Biol.* **151**, 905-918.
Stabach, P. R., Simonovic, I., Ranieri, M. A., Aboodi, M. S., Steitz, T. A., Simonovic, M. and Morrow, J. S. (2009). The structure of the ankyrin-binding site of β-spectrin reveals how tandem spectrin-repeats generate unique ligand-binding properties. *Blood* **113**, 5377-5384
Strunkelnberg, M., de Couet, H. G., Hertenstein, A. and Fischbach, K. F. (2003). Interspecies comparison of a gene pair with partially redundant function: the rst and kirre genes in D. virilis and D. melanogaster. *J. Mol. Evol.* **56**, 187-197.
Tepass, U. (1996). Crumbs, a component of the apical membrane, is required for zonula adherens formation in primary epithelia of *Drosophila*. *Dev. Biol.* **177**, 217-225.
Tepass, U. and Harris, K. P. (2007). Adherens junctions in Drosophila retinal morphogenesis. *Trends Cell Biol.* **17**, 26-35.
Thomas, C. M. and Kiehart, D. P. (1994). Beta heavy-spectrin has a restricted tissue and subcellular distribution during *Drosophila* embryogenesis. *Development* **120**, 2039-2050.
Thomas, C. M., Zarnescu, D. C., Juedes, A. E., Bales, M. A., Londergan, A., Korte, C. C. and Kiehart, D. P. (1998). *Drosophila* betaHeavy-spectrin is essential for development and contributes to specific cell fates in the eye. *Development* **125**, 2125-2134.
Thomas, G. H., Newbern, E. C., Korte, C. C., Bales, M. A., Muse, S. V., Clark, A. G. and Kiehart, D. P. (1997). Intragenic duplication and divergence in the spectrin superfamily of proteins. *Mol. Biol. Evol.* **14**, 1285-1295.
Tomlinson, A. (1985). The cellular dynamics of pattern formation in the eye of *Drosophila*. *J. Embryol. Exp. Morphol.* **89**, 313-331.
Touhara, K., Koch, W. J., Hawes, B. E. and Lefkowitz, R. J. (1995). Mutational analysis of the pleckstrin homology domain of the beta-adrenergic receptor kinase. Differential effects on G beta gamma and phosphatidylinositol 4,5-bisphosphate binding. *J. Biol. Chem.* **270**, 17000-17005.
Vishnu, S., Hertenstein, A., Betschinger, J., Knoblich, J. A., Gert de Couet, H. and Fischbach, K. F. (2006). The adaptor protein X11Lalpha/Dmint1 interacts with the PDZ-binding domain of the cell recognition protein Rst in Drosophila. *Dev. Biol.* **289**, 296-307.
Williams, J. A., MacIver, B., Klipfell, E. A. and Thomas, C. M. (2004). The C-terminal domain of *Drosophila* (beta) heavy-spectrin exhibits autonomous membrane association and modulates membrane area. *J. Cell Sci.* **117**, 771-782.
Wodarz, A., Hinz, U., Engelbert, M. and Knust, E. (1995). Expression of crumbs confers apical character on plasma membrane domains of ectodermal epithelia of Drosophila. *Cell* **82**, 67-76.
Wolff, T. and Ready, D. F. (1993). Pattern formation in the *Drosophila* retina. In *The Development of Drosophila melanogaster*, vol. 2 (eds M. Bate and A. Martinez-Arias), pp. 1277-1325. Plainview: Cold Spring Harbor Laboratory Press.
Zarnescu, D. C. and Thomas, C. M. (1999). Apical spectrin is essential for epithelial morphogenesis but not apicobasal polarity in Drosophila. *J. Cell Biol.* **146**, 1075-1086.
Zhang, P., Talluri, S., Deng, H., Branton, D. and Wagner, G. (1995). Solution structure of the pleckstrin homology domain of Drosophila beta- spectrin. *Structure* **3**, 1185-1195.